FERMILAB $\bar{p}p$ COLLIDER

Alvin V. Tollestrup

This is a report on the status of the Fermilab $\bar{p}p$ collider program. The center of mass energy will be 2 TeV, and preliminary running is being planned for mid 1985. In order for this program to come to fruition, three components must be successfully completed.

1. The Energy Saver
2. $\bar{p}$ Source, consisting of two rings
   a. Debuncher
   b. Accumulator
3. Detectors
   a. CDF B0
   b. D0 (call for proposals early 1983)

The overall layout of the project is shown in Fig. 1. I will now report on the status of each of the individual pieces of the program.

Energy Saver

The Energy Saver is a new 1 TeV ring of superconducting magnets. The sequence of operation is as follows:

1. The booster injects into the main ring as usual, and the main ring accelerates protons to 150 GeV.
2. The protons are extracted from the main ring and injected into the Tevatron.
3. The Tevatron accelerates them in 20 seconds to about 800 GeV. There is a 20 second flat-top and a return ramp of duration of 20 seconds. Thus, the overall

cycle time is one per minute. Either a long spill on the flat-top or fast extraction is being planned.

The status of magnet production is as follows:

Magnet	Number Needed	Number Available 10/22/82
Dipoles	774	802 have been made
66 in. quads	180	245
Special quads	36	

The present status of the installation is as follows:

Sector	Status
A	Three-fourths installed, power tests completed last summer.
B	B0 colliding beam hall being installed.
C	Magnets in place.
D, E	Final leak check.
F	In cooldown.

A very successful power test was completed on Sector A magnets last summer. These tests exercised all of the normal machine control systems in order to cool down the magnets, pulse them, and provide quench protection. The test was extremely successful, and provided the first experience with a large string of superconducting magnets.

Source

Fig. 2 shows a plan of the new source that is being constructed at Fermilab. The Source consists of two rings: A debuncher ring and an accumulator ring, both of which operate at about 8 GeV. Beam is extracted from F17 and brought to bear on a target as soon as it is sufficiently clear of the main ring tunnel. The $\bar{p}$'s produced at the target are collected by a lithium lens and a transport system and injected into the debuncher ring. The debuncher ring interchanges a large momentum spread of the antiprotons and a short time spread for a long time spread and a small momentum spread. In addition, transverse cooling is being planned to reduce the transverse size of the beam. After 2 seconds, the $\bar{p}$'s are extracted from the debuncher and injected into the accumulator. The accumulator utilizes stochastic stacking (à la Van der Meer) as well as transverse cooling during the stacking process. The details of the steps are as follows:

1. One batch of 3×10^{12} protons is accelerated through the booster and the main ring to 120 GeV. At this point, there are 82 bunches of protons which are separated by 20 nanoseconds each.
2. The individual bunch length of the protons is shortened to a sigma of .16 nanoseconds by means of RF manipulations.
3. Protons are extracted from the main ring and focussed to a spot whose sigma is .038 cm at the target.
4. The $\bar{p}$'s are collected by a means of a lithium lens and transported to the debuncher. The emittance of the beam is 20 mm mr in each plane and a $\Delta p/p$ of 4 percent. The total number of $\bar{p}$'s collected per pulse is 7×10^7, and the density of the $\bar{p}$'s is about .2 per electron volt.

5. The very tightly bunched $\bar{p}$'s next undergo a bunch rotation in the debuncher. The initial condition and the conditions 30 turns later are shown in Figs. 3 and 4. The final momentum spread achieved after complete rotation is shown in Fig. 5. The momentum spread has been decreased from 4 percent to .2 percent. As a result, there are now about 5 $\bar{p}$'s per electron volt.
6. Transverse cooling is now applied in each dimension in order to decrease the transverse emittance from 20 π mm mr to less than 7π . This takes about 2 seconds. The process is shown in Fig. 6.
7. The antiprotons are extracted in the debuncher and injected into the accumulator. The accumulator uses stochastic stacking in order to achieve a $\bar{p}$ density 10^5 per electron volt, see Fig. 7. There is also transverse cooling during the stacking process.
8. Finally, the $\bar{p}$'s are extracted from the accumulator, injected into the main ring, accelerated to 150 GeV, transferred to the Tevatron where they are joined with three bunches of protons, and accelerated to full energy.

The design luminosity is 10^{30}, and the Source can supply enough $\bar{p}$'s to achieve this luminosity every two hours after an initial filling time of four hours. The goals of the Source design were to obtain a high luminosity, as well as a high flux of antiprotons. In order to achieve this high flux, it was necessary to go to a stochastic stacking system operating at 1 to 2 GHz. Since the size of the electrodes as well as their spacing from the beam must all be considerably less than a wavelength, it was necessary to reduce the transverse emittance of the beam before injection into the accumulator. After a considerable amount of study, it became apparent that an additional ring, the debuncher ring, was the most economical solution to achieve the initial momentum compaction as well as reduction of transverse emittance. The concept of two separate rings is being copied in the proposal for the new Source at CERN.

An intensive R&D program is being carried out in order to improve the components that are necessary for our Source. For instance, in order to operate at the higher frequencies, it is necessary to construct delay line filters from superconducting delay lines. Low noise wide band amplifiers are particularly advantageous for the transverse cooling in the debuncher. Cryogenically cooled amplifiers are being developed for this purpose. Wide band loop-couplers become increasingly difficult to construct as a frequency is raised, and an intensive R&D program is underway on this subject. We are also investigating the nonlinearities inherent in travelling wave tubes since these cause unwanted heating of the beam. The effect can be reduced by operating the TWT's at a small fraction of their rated power. However, this becomes an important economic consideration in designing a high power cooling system since tubes are very expensive. Finally, intensive R&D is underway on the lithium lens which collects the $\bar{p}$'s from the target.

A rough schedule for this project is as follows: The Saver commissioning will start in the spring of 1983 and continue until the fall, at which point there will be a fixed target run for physics that will occupy from the fall of 1983 and the spring of 1984. There will then be a short shutdown to fix troubles that have developed during this running period and to install new features as experience will indicate. There will then be an eight month full energy TeV II run for fixed target physics. In mid-1985, there will be a one-month long TeV I Source and detector run, after which the machine will be shut down to construct D0 and the overpass at B0 which carries the main ring beam around the detector. The first major physics run for TeV I will take place starting in the summer of 1986. At this point, I estimate that the integrated luminosity at CERN will be a few times 10^{36}.

Detector

The collider program calls for two experimental halls. One at B0, which is at the present under construction, and a second at D0, which will be built later. A bypass to shunt the main ring beam over the detector at B0 is being planned. At present, B0 is under construction and is even somewhat ahead of schedule. All of the concrete work for the assembly halls and the collision hall have been completed, and the above ground building is under construction. We have been fortunate in having a mild winter at Fermilab, and the contractor has made optimum use of this opportunity. Figs. 8 and 9 show the collision and the assembly hall. The length along the beam is greater than available at CERN due to the higher collision energies that we anticipate.

Proposals for the D0 collision area will be considered in the spring of 1983. The design of the collision hall will be dependent on the proposals that are accepted. Hence, in the rest of this talk, I will concentrate on the detector that is being constructed for the B0 hall.

The Design Report was completed August 1981. The members of the collaboration at that point are shown in Fig. 10. Since the Design Report was completed, three new institutions have joined the collaboration in June 1982.

The design goal was to construct a detector that would do the physics of quarks, gluons, and leptons over the largest possible part of the rapidity range. This required high granularity with the electromagnetic and hadron calorimetry which is all in the form of towers that project back toward the collision point. The central electromagnetic and hadron calorimetry is done by means of scintillation plastic whereas the rest of the calorimetry is by means of proportional tubes. Charged particle tracking is provided between 2^{o} and 178^{o}, and precision momentum measurement is provided in the central region by means of a 3 meter diameter x 5 meter long superconducting solenoid operating at 1.5 Tesla. In addition, there are toroids in the forward and backward direction for the measurement of muon momentum. Fig. 11 shows the overall resolution of the calorimetry. The squares are the individual cells, and the dotted ellipses are the size of a typical QCD jet.

The following Figs. 12-16 compare cross sections at CERN and at Fermilab for several processes. In some cases, I have drawn a line that crosses at a level equal to a luminosity of 10^{36}. I've done this for two reasons: The first is that it indicates approximately the level that I believe CERN will have achieved by the time the collider at Fermilab starts to operate, and second, with a luminosity of 10^{30}, it is reasonable to expect an integrated luminosity of 10^{36} in any individual run. I believe we can expect this kind of luminosity or even a factor of 10 higher within the next few years.

Fig. 16 shows the total cross section for associated $\bar{t}t$ production. For a $\bar{t}$ mass near 25 GeV, an integrated luminosity of 10^{36} gives 6 x 10^4 events. If a $\bar{t}$ quark decays via flavor cascade, we can arrive at a situation that approximates three jets, provided there are no semileptonic decays in the chain. For instance, if a $\bar{t}$ goes into a W^+ and b, the b will decay via its flavor cascade into an approximation of a single jet since none of the particle masses are very high. If a W decays into a u and d, we will then have three jets. If the associated t decayed into a b and a W^-, which in turn decayed leptonically, we would have opposite the t a single jet event with a high energy lepton. We consider the case where we can trigger on the high energy lepton and try to reconstruct the t mass from its associated three jets. This type of topology has been described in detail in a CDF report, CDF-70. The efficiency of reconstruction is not high. However, Monte Carlo studies indicate that it should be possible to isolate such events.

A mass reconstruction using the calorimetry information only of the three jets is shown in Fig. 17. One hundred events out of the original 6 x 10^4 have survived all of the cuts, the most serious of which is a p_t cut of greater than 50 GeV for the three jets.

We will now proceed to a description of the individual components of the detector. An overall drawing of the detector is shown in Fig. 18. In addition, Fig. 19 and Table 1 indicates the properties of the detector in the various angular regions.

The present status of the calorimetry is as follows: All of the components have had prototypes constructed and tested in beams. Fig. 20 shows a 15^o wedge from the central calorimetry. Fig. 21 shows its segmentations in rapidity. The front part of the module consists of a lead scintillator sandwich with a strip chamber embedded at shower maximum for position information. The next section consists of 1 inch steel plates with scintillators embedded and read out by shifter bars. The last section at the back houses the muon tracker.

The steel for the modules has been cut using a computer controlled plasma cutter in a shop at Purdue. The great number of different shapes of scintillator for the hadron calorimeter have been cut with a computer control laser facility at Frascati, and an assembly line to wrap the scintillator and fabricate the light shifters has been set up at Pisa (see Fig. 22a). The electromagnetic towers are being fabricated at Argonne as well as the strip chambers which are located at shower maximum to give position information (see Fig. 22b). The scintillator and shifter for this calorimeter was developed in Japan. The muon tracking system is being fabricated at Urbana. All of these components will come together in an assembly line that is being constructed at Fermilab and which will come into operation in the summer of 1983. One complete wedge module was tested in the beam before the design was finalized.

The endwall hadron calorimetry modules are now starting to be constructed. Again, the plates for this unit are fabricated using a plasma cutter under computer control.

The forward endplug calorimetry is also now under construction. The electronic part is constructed of lead sheets interspersed with resistive plastic tube chambers and with pad and strip readout as well as segmentation in depth. These chambers are the responsibility of Tsukuba University. The hadron calorimetry section consists of 5 cm thick steel plates interspersed with resistive tube proportional chambers with pad readout and is the responsibility of LBL. The pads of these two sets of chambers are arranged in the form of projective towers. This part of the calorimtry was particularly difficult to design because it is also part of the magnetic circuit, and the forces are very high. Fig. 23 shows a view of one section of the endplug with its associated calorimetry. Fig. 24 shows an exploded view of the chambers in the electromagnetic section, and Fig. 25 and 26 show the response of the electromagnetic calorimeter to 100 GeV π^- and e^-, respectively. These plots are made on the basis of beam measurements.

The magnet is a superconducting solenoid that is 3 meters in diameter and 5 meters long, and it is presently being constructed by Hitachi in Japan. Preliminary design and specifications for this coil were made by a collaboration of Tsukuba University and Fermilab. The coil is scheduled for completion this year and will be delivered to Fermilab for magnetic tests in 1984.

The parts of the detector that I have described up until now are the most advanced in their construction phase. This is because some of the calorimetry is integral with the magnet return circuit and, hence, must be completed before magnet tests can be carried out. Some of these components also had an influence on the design of the B0 collision hall and assembly area, and hence their design had to proceed at a rather rapid pace in order to insure compatability between the building and the detector.

The central tracking system is still under study, although detailed model tests have been carried out on one proposed system which consists of ten sets of half staggered double planes. In addition, there are five u and five v planes giving a total of 20 radial planes of tracking. The wires are in the z direction and typical cells are shown in Fig. 27. An overall view of the central chamber is shown in Fig. 28. The concave end supports allow adequate wire tension with a minimum thickness of material in the way of the particles. Two other tracking systems in the central region are under study. The first is a silicon vertex detector that would fit very close around the beam pipe. The second is a tracking system that would be useful for angles smaller than that which the central tracking chamber covers.

All of the calorimetry and tracking so far described are attached to the magnet and move in and out of the assembly hall. A 10^{o} hole in the wedge allows particles in this angular region to proceed into the forward and backward calorimetry and tracking systems. These systems are fixed in place and do not roll in and out. These systems are symmetrical in the forward and backward direction and allow for electrical and hadron calorimetry as well as muon tracking. The electromagnetic calorimetry is being constructed at Harvard; the hadron calorimetey is being constructed at Texas A&M, and the muon toroids and tracking system are being constructed at Wisconsin..

The data acquisition system must handle over 75,000 channels. It must be simple, reliable, and inexpensive. Many components of this system are presently being designed and tested. However, the basic architecture of this system has been settled. The high level CPU will be a VAX, and the various processors in the system will be linked by means of FASTBUS. Much of the front end electronics will be placed on the detector since we are relying on a fast regeneration time in the Source to make the detector easily available in case of malfunction in the collision hall. Finally, it has been decided that the major means of communicating of data between the detector and the electronics house will be done by means of DC analog signals. A block diagram of this system is shown in Fig. 29. The position of the various electronics components relative to the shielding wall is also indicated in this diagram. The system may be subdivided into small sections for trouble shooting. The processors that control all the subsystems are tied to the VAX CPU by means of FASTBUS.

A typical channel of front end electronics is shown below:

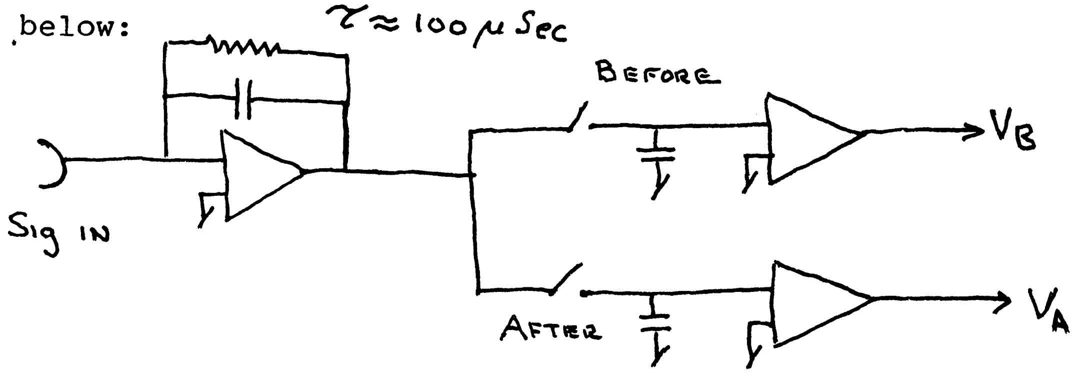

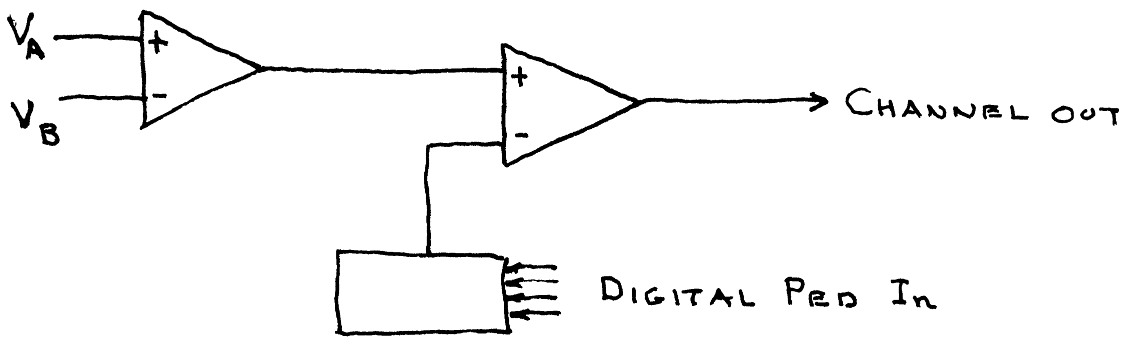

The signal coming in from a wire, a pad, or a phototube is integrated in a charge sensitive amplifier and stretched to the order of 100 microseconds. The two switches labelled "before" and "after" are actuated before the beam crossing and after the beam crossing. The difference of these two times forms a gate for the experiment, and the two signals from the sample and hold amplifiers are then subtracted in a difference amplifier to give the channel out. In the case of no event, the condensers are reset before the next crossing.

The function of the trigger is to keep the condensers from being reset and to keep the "before" and "after" switches open. The event is thus stored in analog fashion until it is read out in the next few milliseconds. The drift in the sample and hold system is small enough so that this can be done quite accurately. The individual channels are scanned under computer control, and the analog signal is sent from the detector to the electronics house. This system results in an enormous reduction of the number of cables that must connect the detector with the rest of the data acquisition system. It has the disadvantage that a considerable amount of complex electronics is installed at the detector, and hence, not accessible during a store.

The trigger is broken up into three levels. Level 1, the lowest level, operates from analog signals sent from the detector. The Level 2 trigger utilizes this analog information in a more sophisticated way to find clusters or other interesting configurations from the calorimetry information. Finally, a very sophisticated Level 3 trigger utilizing all digital information controls the data logging operation.

Many components of this system have been built and tested. There is an enormous amount of work left to do on both the front end electronics and on the FASTBUS components. The intention is to get the major components of the system built by industry after the initial development phase is finished.

Finally, I would like to finish by showing some of the events from our simulation program. Since the field is axial along the beam, the event display is considerably different in appearance than the ones we have seen from UA1. Fig. 30 shows a typical high p_t event in three views. Fig. 31 shows an expanded view of the vertex of the same event. Figs 32 and 33 show the same event with a p_t cut of 1 GeV.

This conference has been historic in that it has exposed the richness of the physics that underlies high energy $\bar{p}p$ collisions. The world is really composed of quarks, gluons, and leptons! The sophistication and granularity in our detector is sufficient to do an excellent job of analyzing this type of physics. We look forward with great anticipation to the day when we can join you in analyzing real data instead of Monte Carlo events.

COLLIDER PLAN

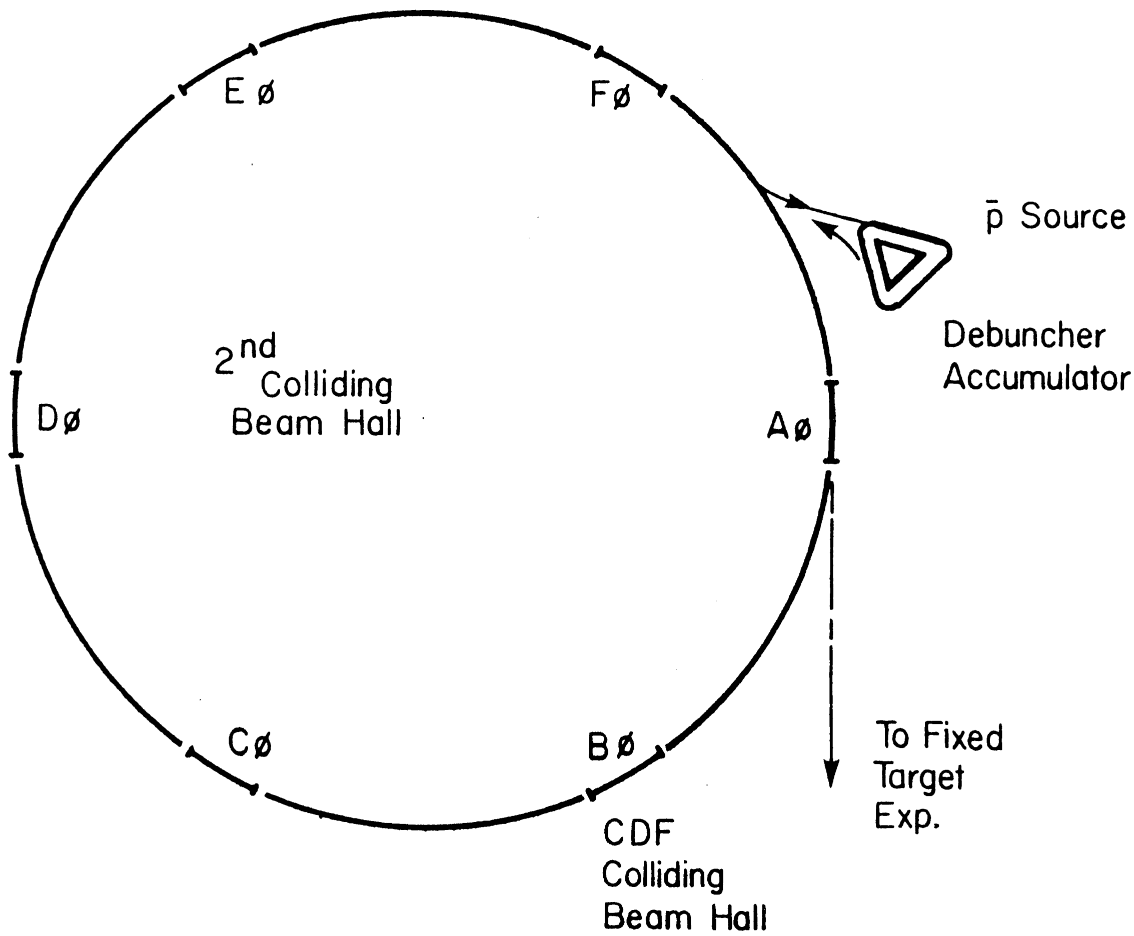

Fig. 1

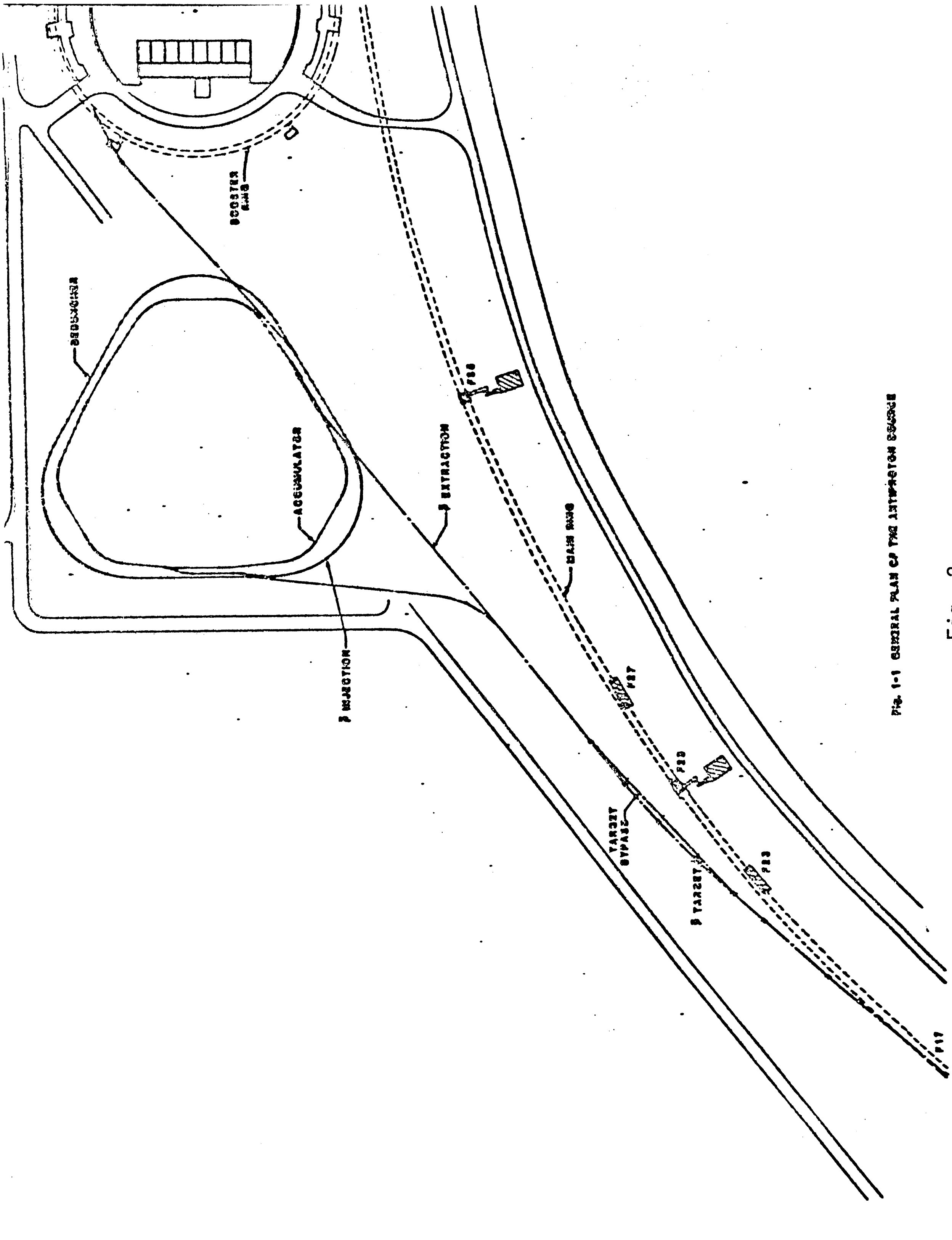

Fig. 1-1 GENERAL PLAN OF THE ANTIPROTON SOURCE

Fig. 2

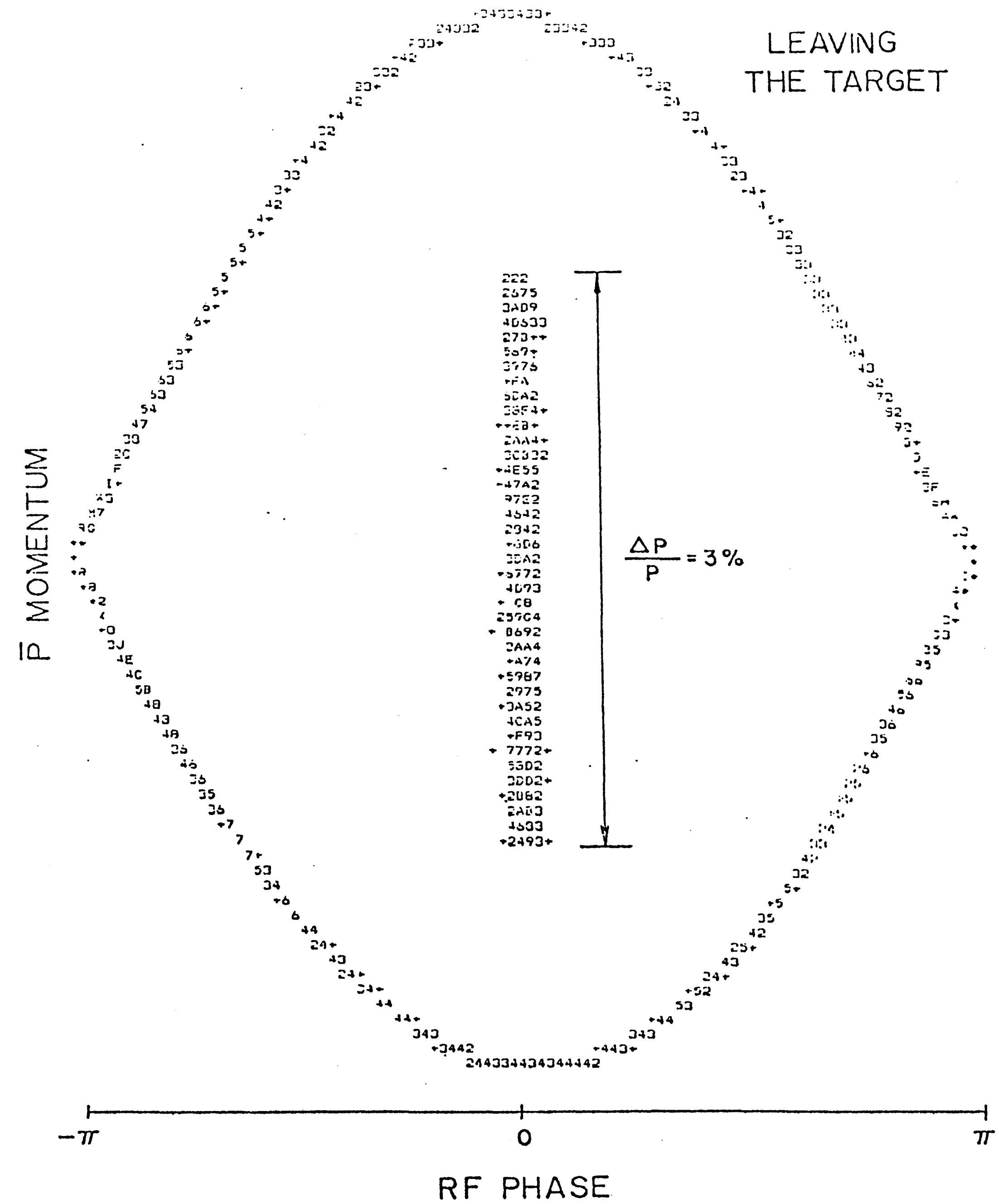
LEAVING
THE TARGET
$\frac{\Delta P}{P} = 3\%$
$\bar{P}$ MOMENTUM
$-\pi$
0
π
RF PHASE

Fig. 3

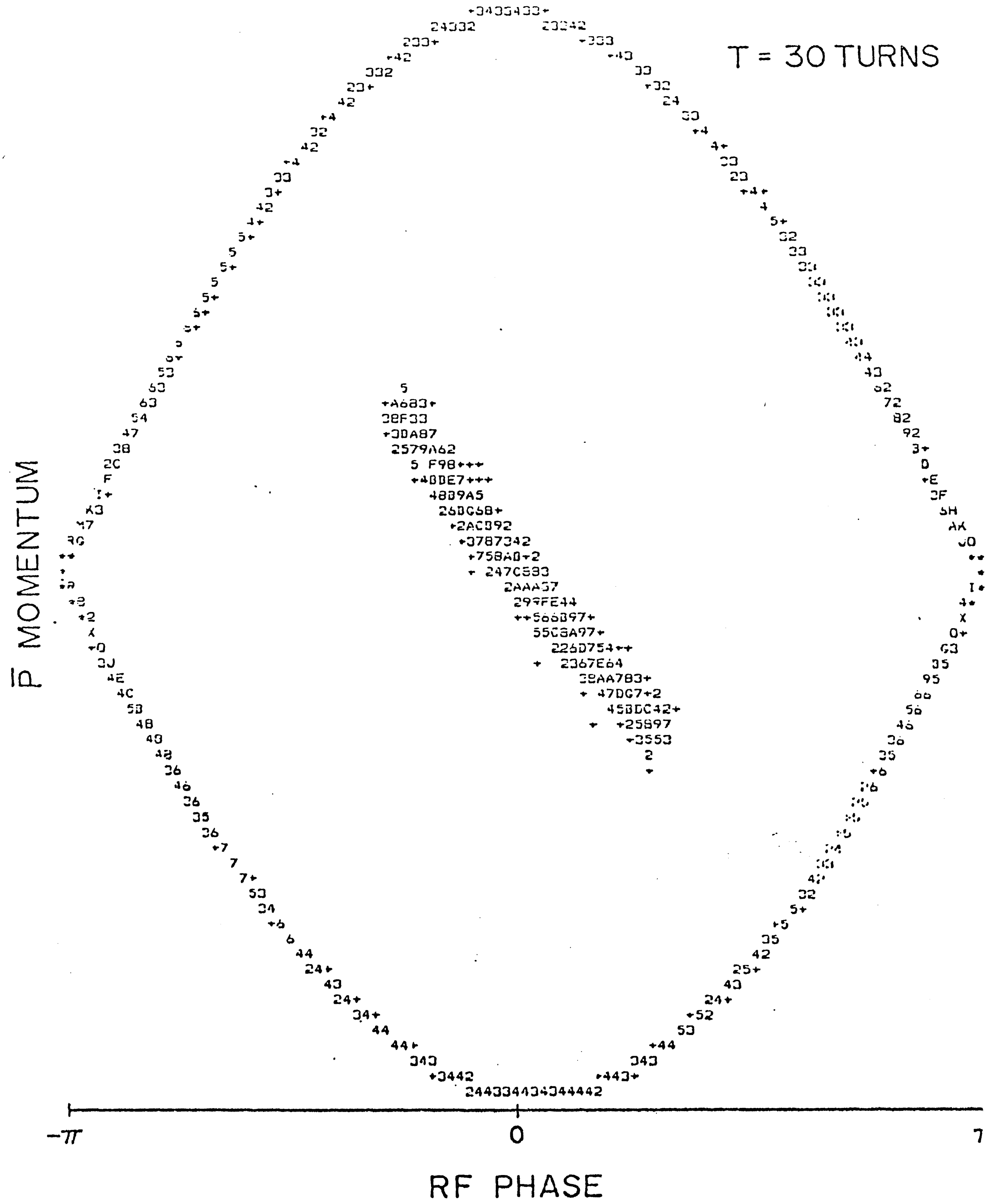

Fig. 4

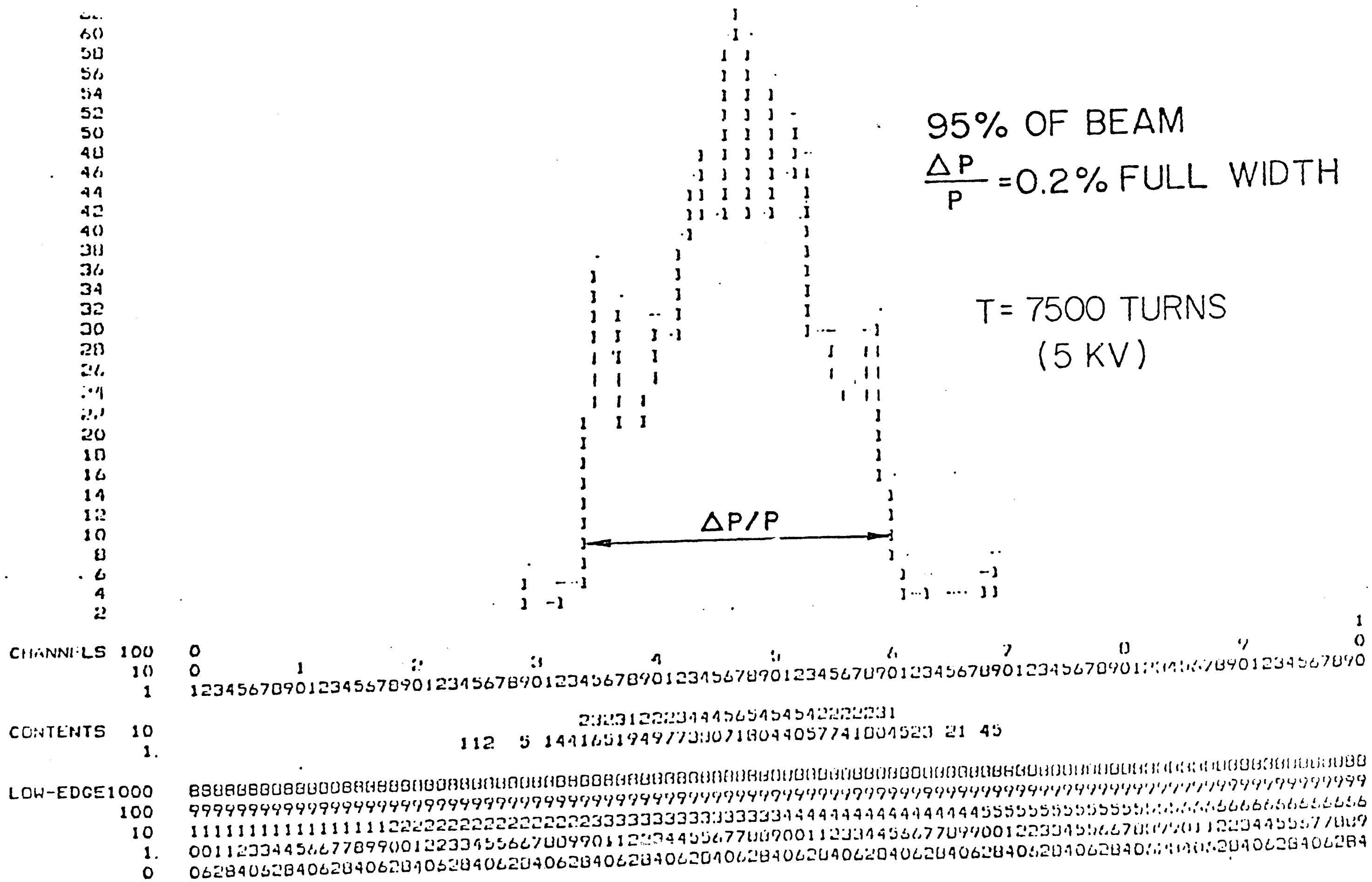

95% OF BEAM
ΔP/P =0.2% FULL WIDTH
T= 7500 TURNS
(5 KV)
ΔP/P
CHANNELS
CONTENTS
LOW-EDGE

Fig. 5

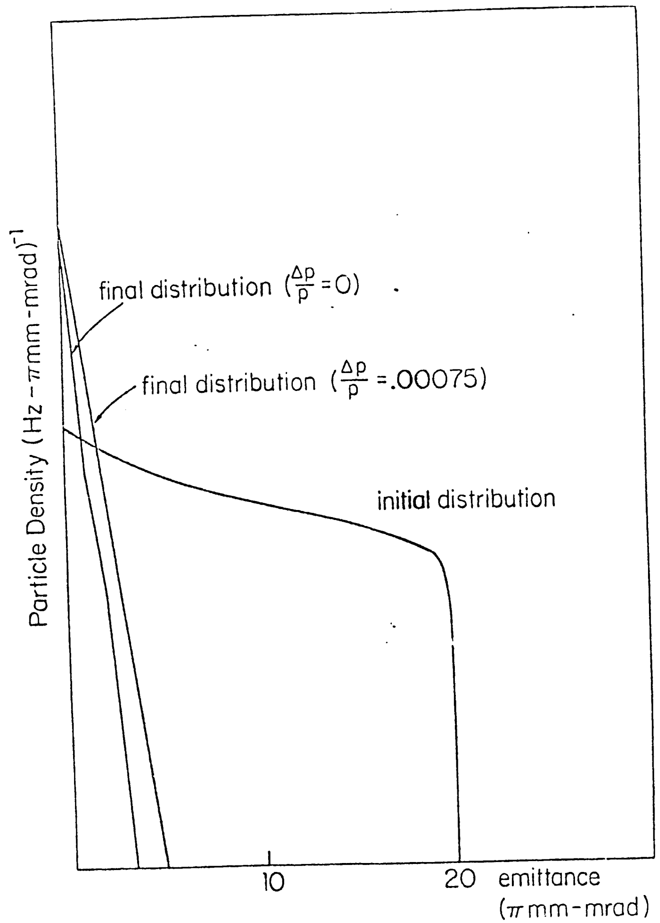
Particle Density (Hz - π mm-mrad)^-1
final distribution (Δp/p = 0)
final distribution (Δp/p = .00075)
initial distribution
10
20
emittance
(π mm-mrad)

Fig. 6

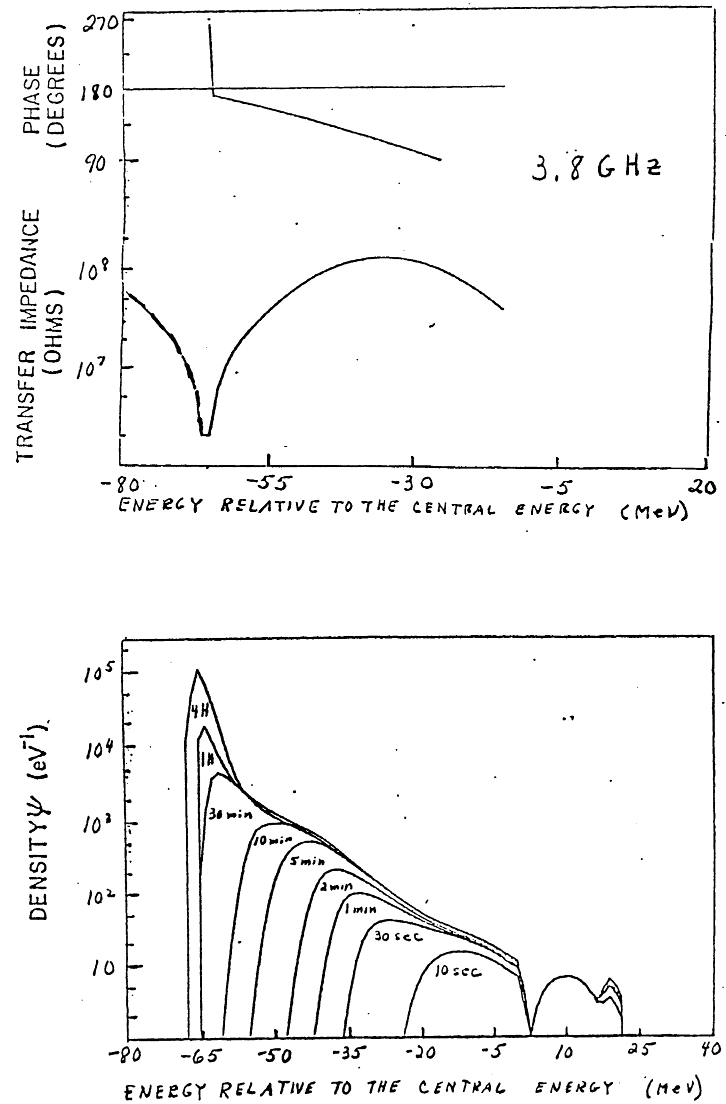
PHASE
(DEGREES)
270
180
90
3.8 GHz
TRANSFER IMPEDANCE
(OHMS)
10^8
10^7
-80
-55
-30
-5
20
ENERGY RELATIVE TO THE CENTRAL ENERGY (MeV)
DENSITY ψ (eV^-1)
10^5
10^4
10^3
10^2
10
4H
1H
30 min
10 min
5 min
2 min
1 min
30 sec
10 sec
-80
-65
-50
-35
-20
-5
10
25
40
ENERGY RELATIVE TO THE CENTRAL ENERGY (MeV)

Fig. 7

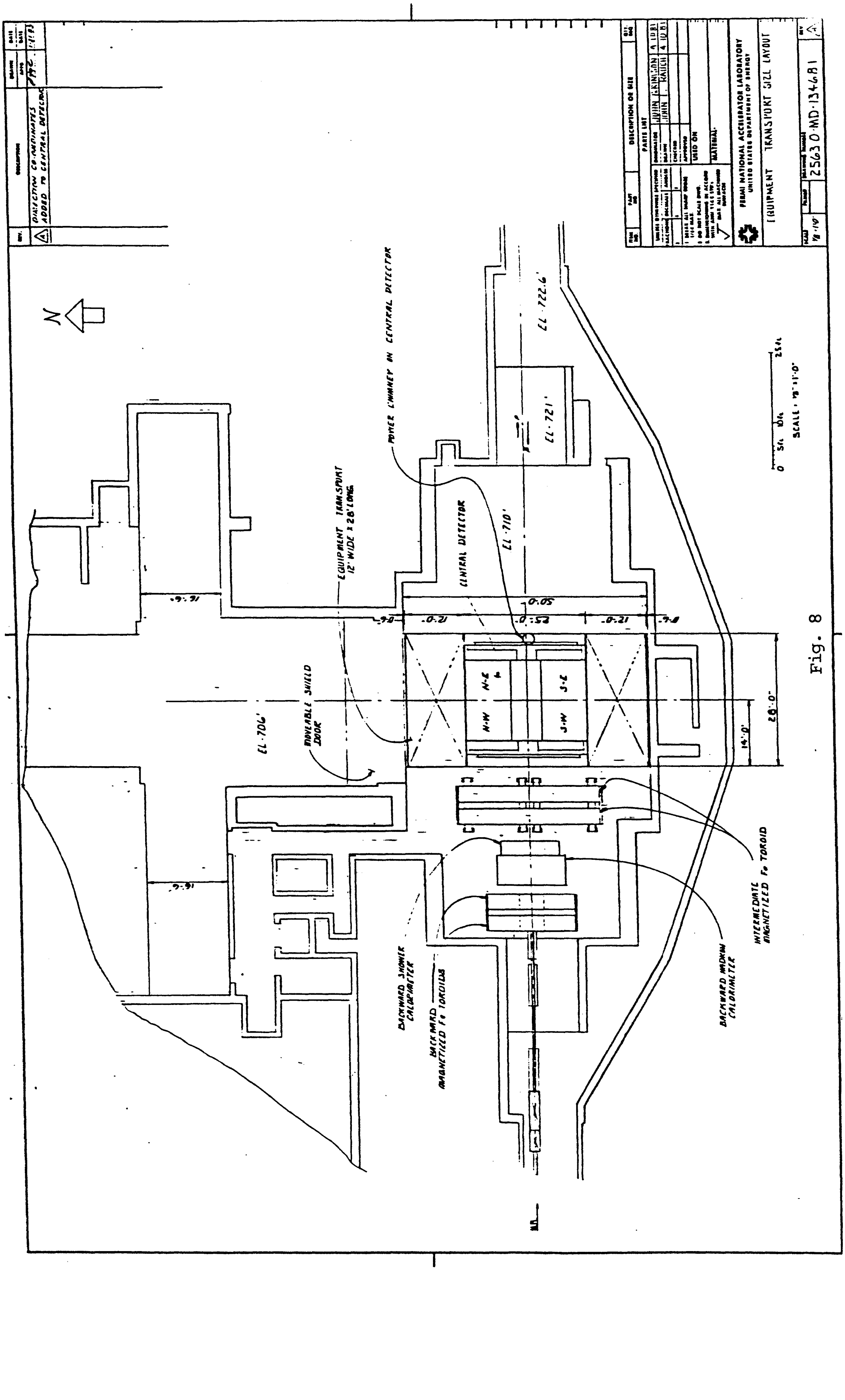

N
EL 706'
EL 710'
EL 721'
EL 722.6'
CENTRAL DETECTOR
EQUIPMENT TRANSPORT
12' WIDE x 28' LONG
POWER CHIMNEY IN CENTRAL DETECTOR
MOVEABLE SHIELD DOOR
N-W
N-E
S-W
S-E
14'-0"
28'-0"
BACKWARD SHOWER CALORIMETER
BACKWARD MAGNETIZED Fe TOROIDS
INTERMEDIATE MAGNETIZED Fe TOROID
BACKWARD HADRON CALORIMETER
DIRECTION CO-ORDINATES ADDED TO CENTRAL DETECTOR
FERMI NATIONAL ACCELERATOR LABORATORY
UNITED STATES DEPARTMENT OF ENERGY
EQUIPMENT TRANSPORT SIZE LAYOUT
25630-MD-134681

Fig. 8

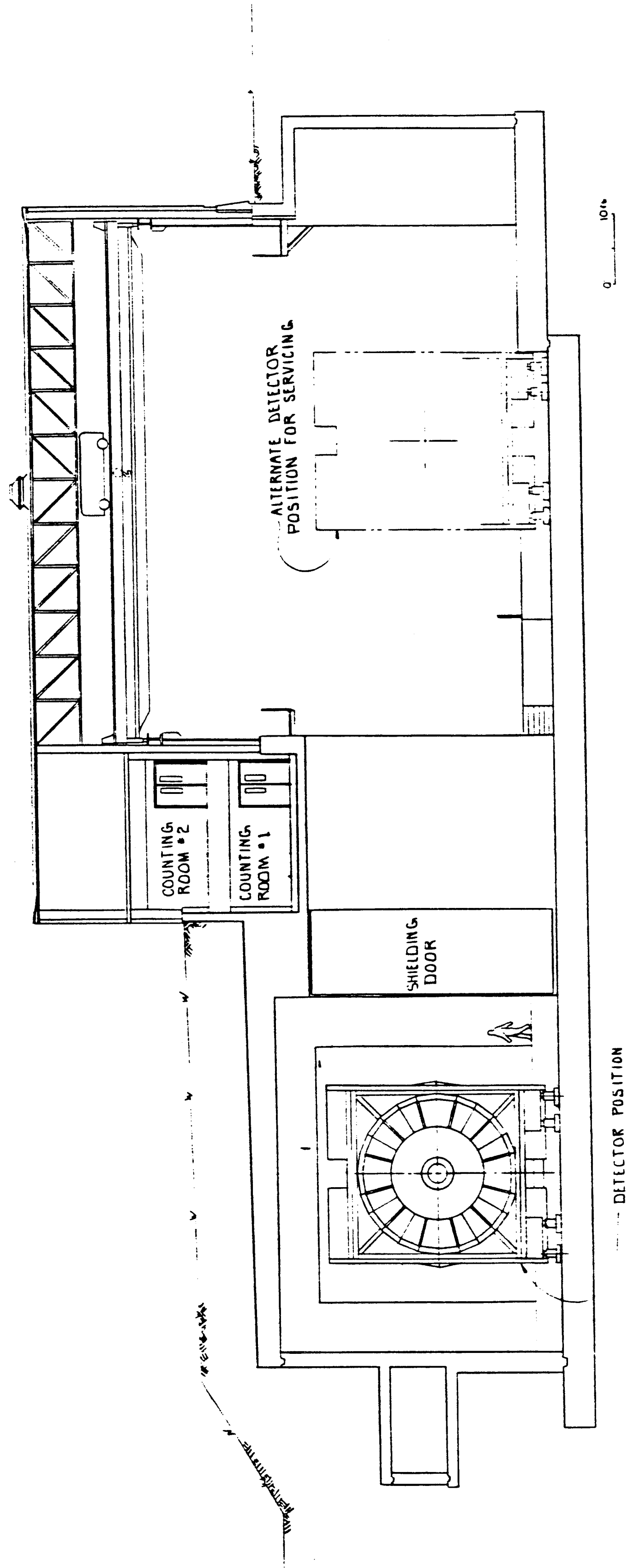
ALTERNATE DETECTOR
POSITION FOR SERVICING
COUNTING
ROOM #2
COUNTING
ROOM #1
SHIELDING
DOOR
DETECTOR POSITION
ON BEAM LINE
0

Fig. 9

DESIGN REPORT

For the Fermilab Collider Detector Facility (CDF)

Argonne National Laboratory - D. Ayres, R. Diebold, E. May, B. Musgrave, L. Nodulman, J. Sauer, R. Wagner, A. B. Wicklund

University of Chicago - H. Frisch, C. Grosso-Pilcher, M. Shochet

Fermi National Accelerator Laboratory - M. Atac, F. Bedeschi, A. Brenner, T. Collins, T. Droege, J. Elias, J. Freeman, I. Gaines, J. Grimson, D. Gross, D. Hanssen, H. Jensen, R. Kadel, H. Kautzky, R. Kephart, T. Ohska, M. Ono, R. Thatcher, D. Theriot, A. Tollestrup, K. Turner, R. Yamada, J. Yoh

Laboratori Nazionali dell' INFN - Frascati - S. Bertolucci, M. Cordelli, P. Giromini, P. Sermoneta

Harvard University - G. Brandenburg, R. Schwitters

University of Illinois - G. Ascoli, B. Eisenstein, L. Holloway, U. Kruse

KEK - S. Inaba, M. Mishina, K. Ogawa, F. Takasaki, Y. Watase

Lawrence Berkeley Laboratory - W. Carithers, W. Chinowsky, R. Kelly, K. Shinsky

University of Pisa - G. Bellettini, R. Bertani, L. Bosisio, C. Bradaschia, R. DelFabbro, E. Focardi, M. A. Giorgi, A. Menzione, L. Ristori, A. Scribano, G. Tonelli

Purdue University - V. Barnes, R. S. Christian, C. Davis, A. F. Garfinkel, A. Laasanen

Texas A&M - P. McIntyre, T. Meyer, R. Webb

Tsukuba University - Y. Asano, S. Kim, K. Kondo, S. Miyashita, H. Miyata, S. Mori, I. Nakano, Y. Takaiwa, K. Takikawa, Y. Yasu

University of Wisconsin - D. Cline, R. Loveless, R. Morse, L. Pondrom, D. Reeder, J. Rhoades, M. Sheaff

Three new institutions, Spokesman in parentheses, joined the collaboration in June 1982: Brandeis University (Jim Bensinger), University of Pennsylvania (H. H. Williams), and Rutgers University (Tom Devlin).

Fig. 10

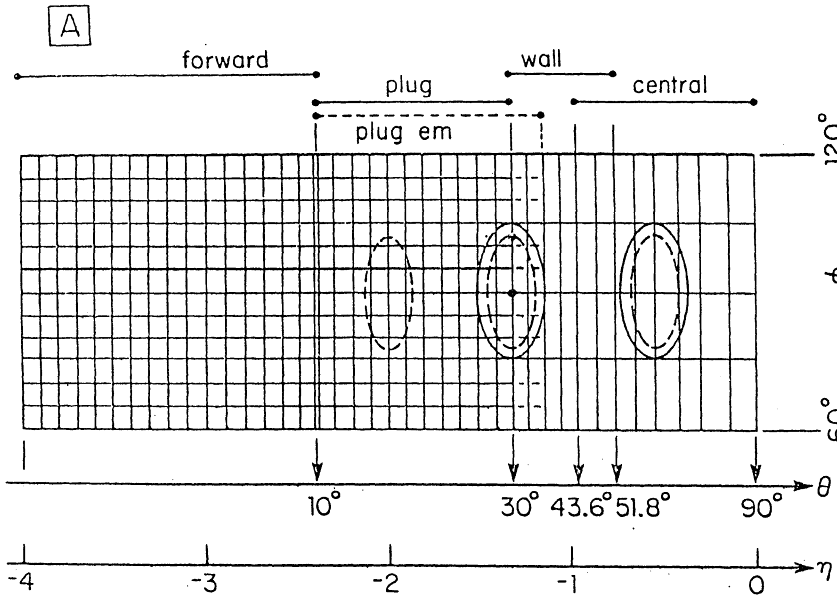

Fig. 11

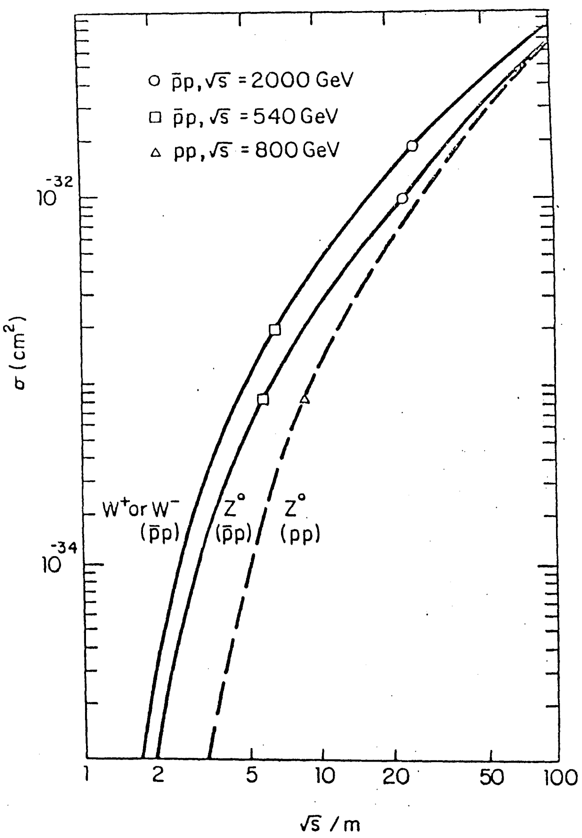

Fig. 12

Fig. 13

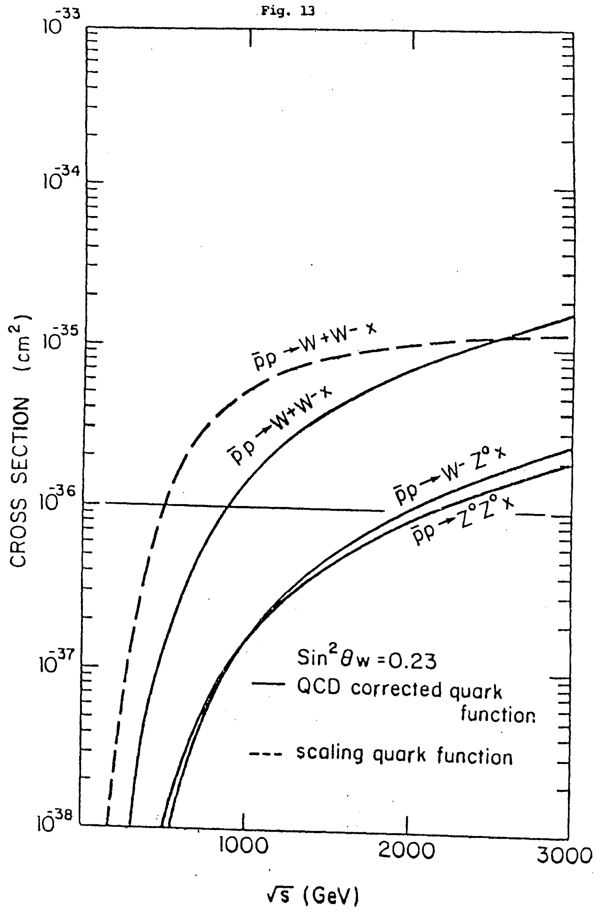

Fig. 14

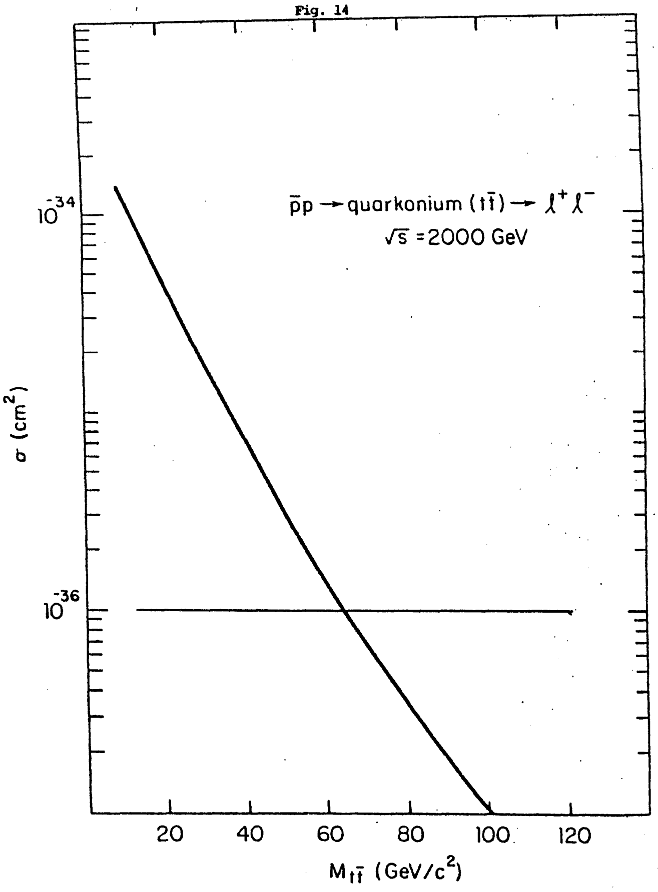

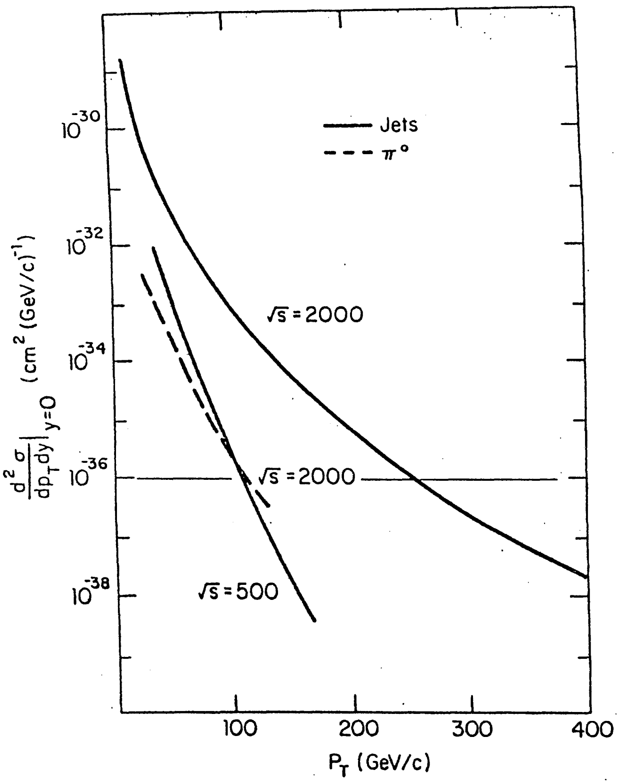

Fig. 15

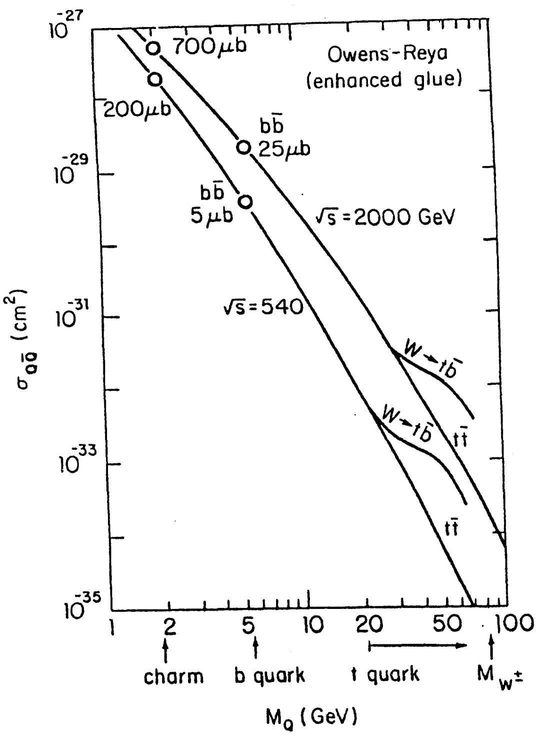

Fig. 16

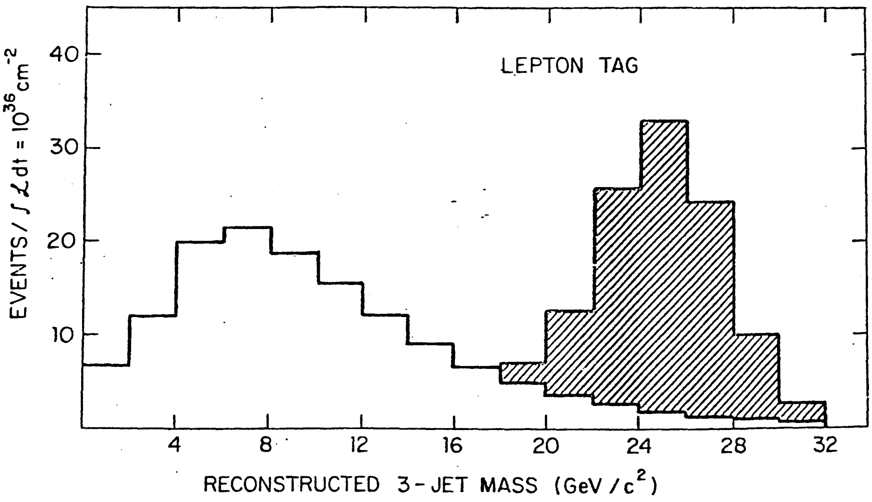
LEPTON TAG
EVENTS / ∫ ℒ dt = 10^36 cm^-2
10
20
30
40
4
8
12
16
20
24
28
32
RECONSTRUCTED 3-JET MASS (GeV/c^2)

Fig. 17

Fig. 18

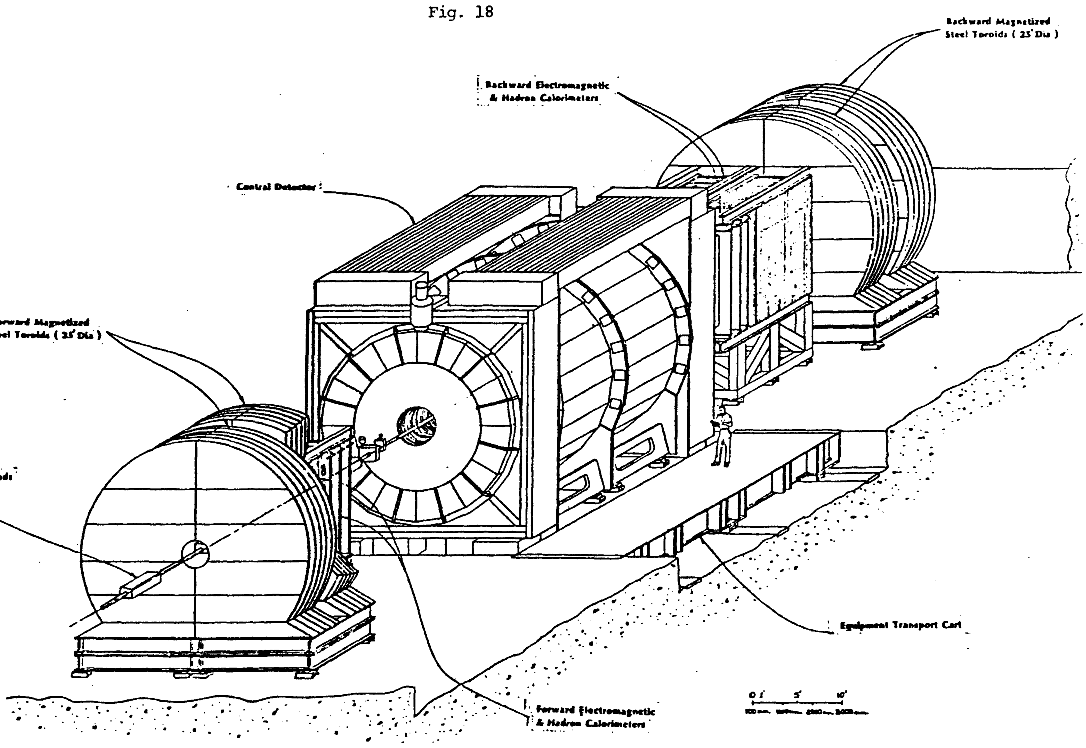
Backward Magnetized Steel Toroids (25' Dia)
Backward Electromagnetic & Hadron Calorimeters
Central Detector
Forward Magnetized Steel Toroids (25' Dia)
Low Beta Quads
Equipment Transport Cart
Forward Electromagnetic & Hadron Calorimeters
0' 5' 10'

Table 1

EM SHOWER COUNTERS			
Property	Central	Plug	Forward
Sampling medium	Scintillator	MWPC	MWPC
Thickness	$17 X_o$	$21 X_o$	$23 X_o$
$1/2 \times (\theta$-range)	36°-90°	10°-37°	2°-10°
Element size $\Delta\phi \times \Delta\eta$	15°×0.1	5°×0.1	5°×0.1
σ_E/E	$15\%/\sqrt{E}$	$25\%/\sqrt{E}$	$25\%/\sqrt{E}$
$\sigma_{x,y}$ (E>50 GeV)	~3mm	~1mm	~1mm
Hadron rejection	$\sim 10^3$	$\sim 5\times10^2$	few $\times 10^2$

Hadron Calorimeters				
Property	Central	Wall	Plug	Forward
Sampling medium	Scintillator	Scintillator	MWPC	MWPC
Λ_{Fe} Perpendicular	5Λ	4.4Λ	6Λ	8.3Λ
$1/2 \times (\theta$-range)	40°-90°	30°-50°	10°-30°	2°-10°
Element size $\Delta\phi \times \Delta\eta$	15°×0.1	15°×0.1	5°×0.1	5°×0.1
σ_E/E	$5\% + \frac{62\%}{\sqrt{E}}$	$\sim \frac{90\%}{\sqrt{E}}$	$\sim \frac{100\%}{\sqrt{E}}$	$\sim \frac{100\%}{\sqrt{E}}$
$\sigma_{x,y}$	~5cm	~5cm	~1cm	~1cm

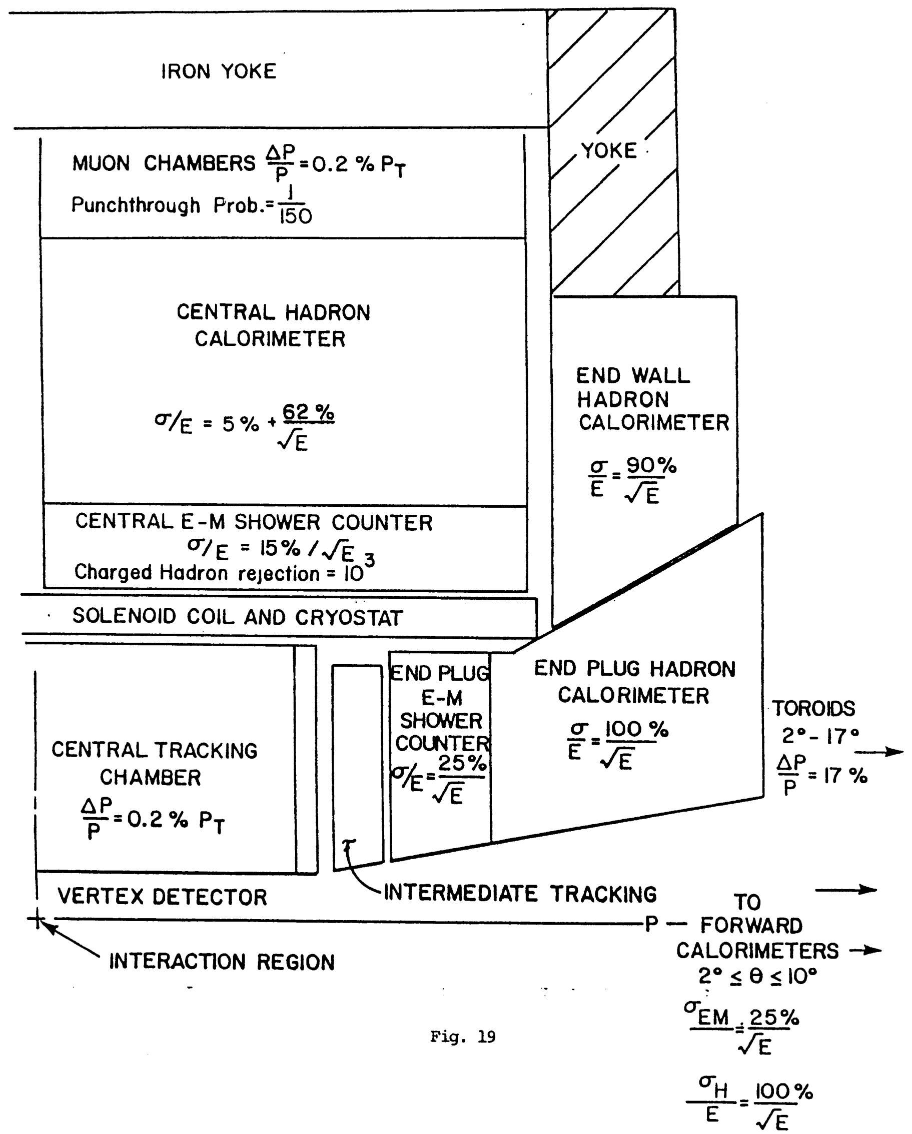

Fig. 19

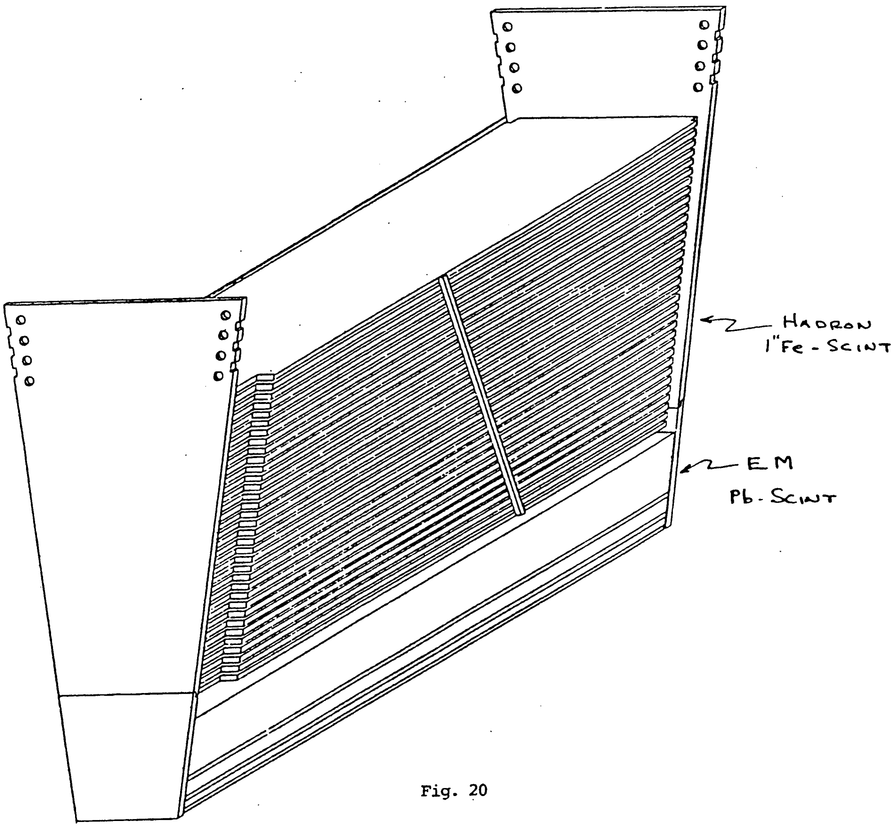
HADRON
1"Fe - SCINT
EM
Pb - SCINT

Fig. 20

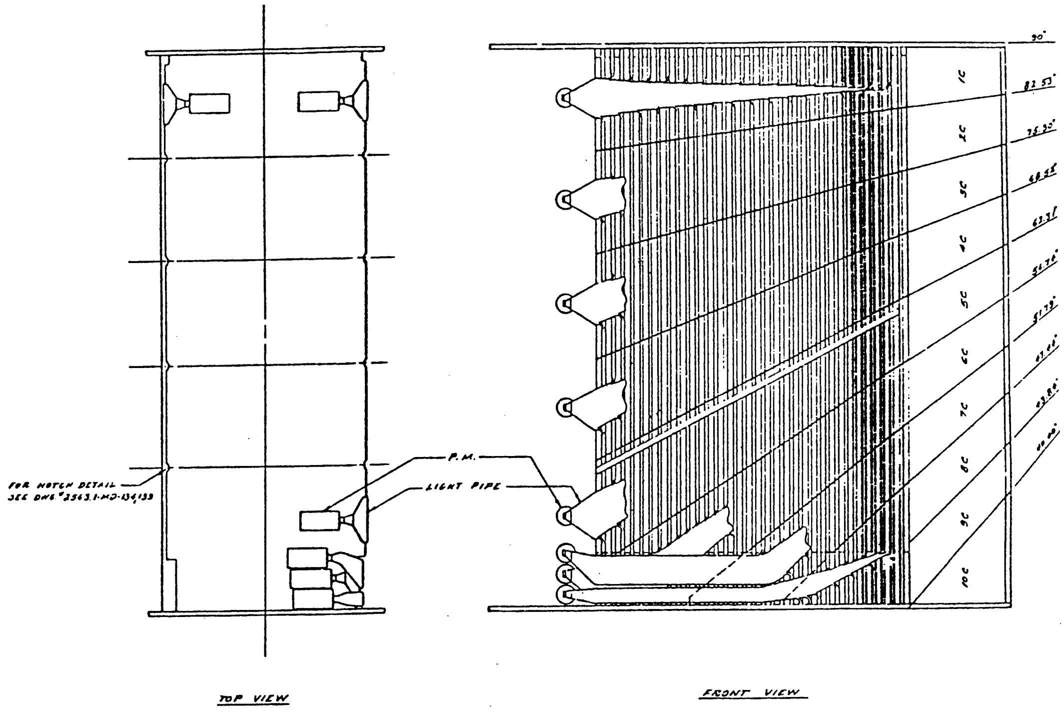
P.M.
LIGHT PIPE
TOP VIEW
FRONT VIEW

Fig. 21

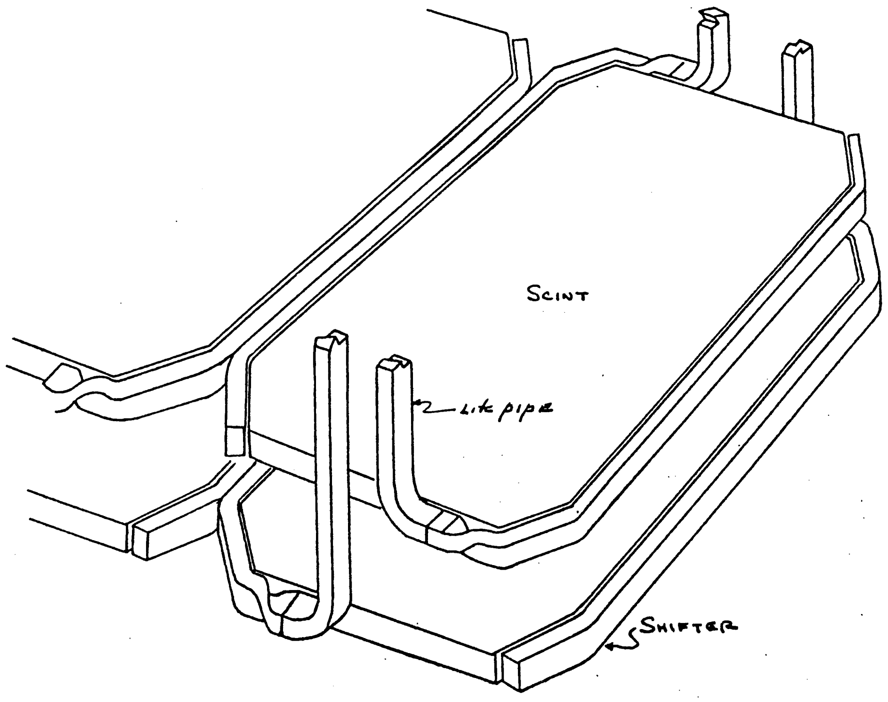

Fig. 22a

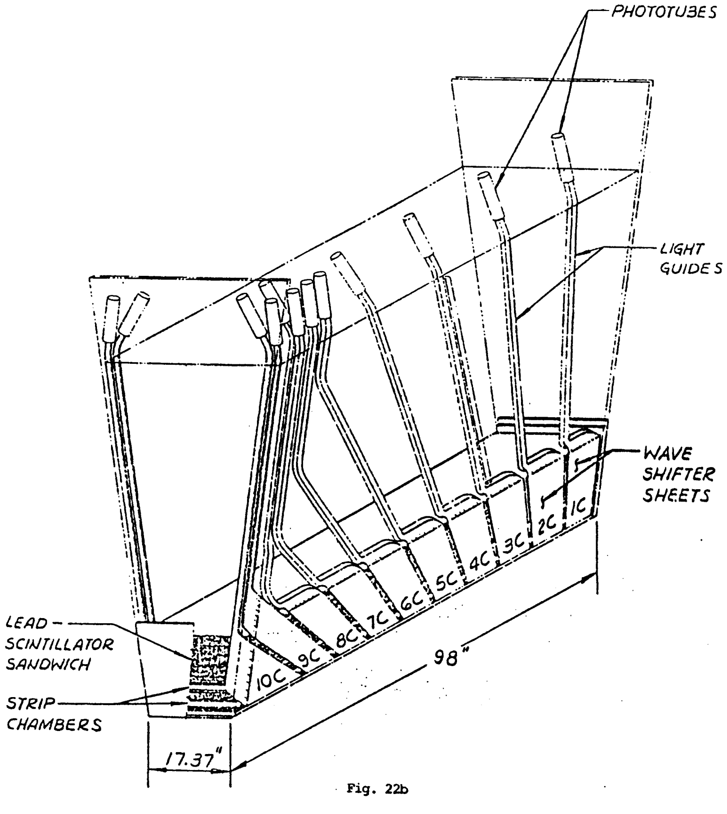

Fig. 22b

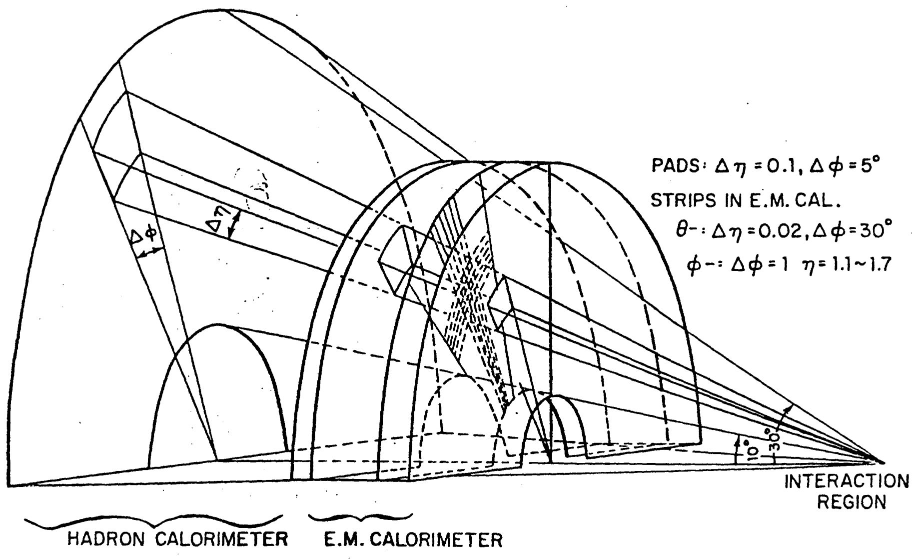
PADS: Δη = 0.1, Δφ = 5°
STRIPS IN E.M. CAL.
θ-: Δη = 0.02, Δφ = 30°
φ-: Δφ = 1 η = 1.1~1.7
Δφ
Δη
10°
30°
INTERACTION REGION
HADRON CALORIMETER
E.M. CALORIMETER

Fig. 23

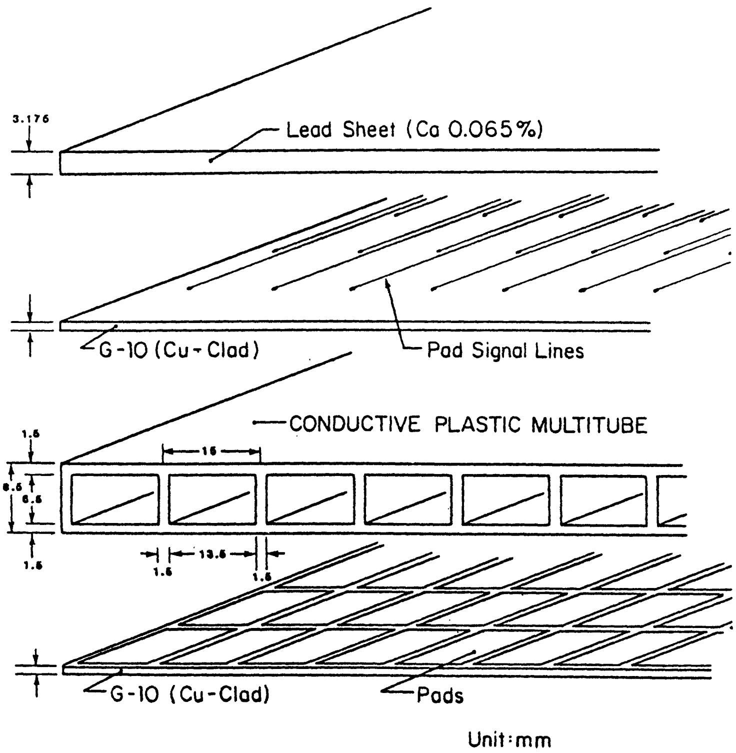
3.176
Lead Sheet (Ca 0.065%)
G-10 (Cu-Clad)
Pad Signal Lines
CONDUCTIVE PLASTIC MULTITUBE
1.6
15
6.5
1.6
13.5
1.6
1.6
G-10 (Cu-Clad)
Pads
Unit: mm

Fig. 24

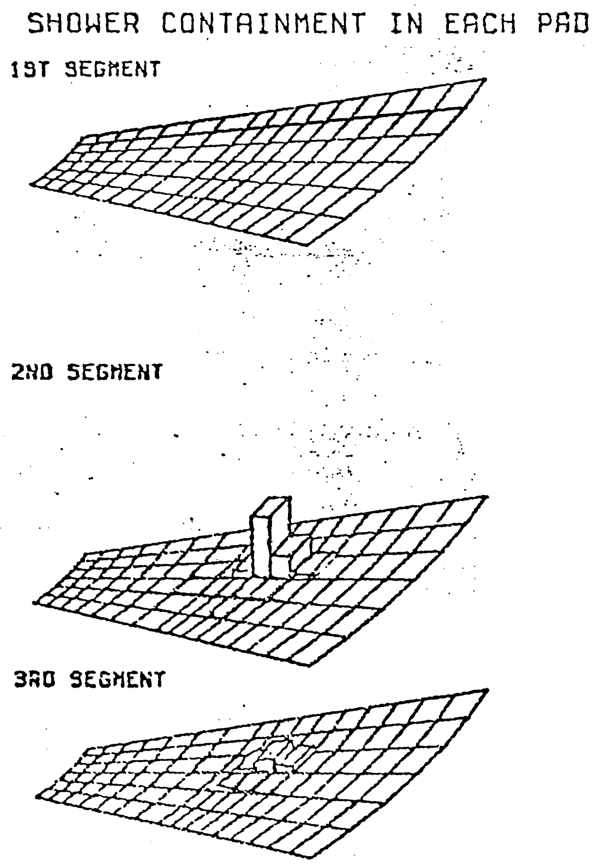

100 GeV e^-

Fig. 25

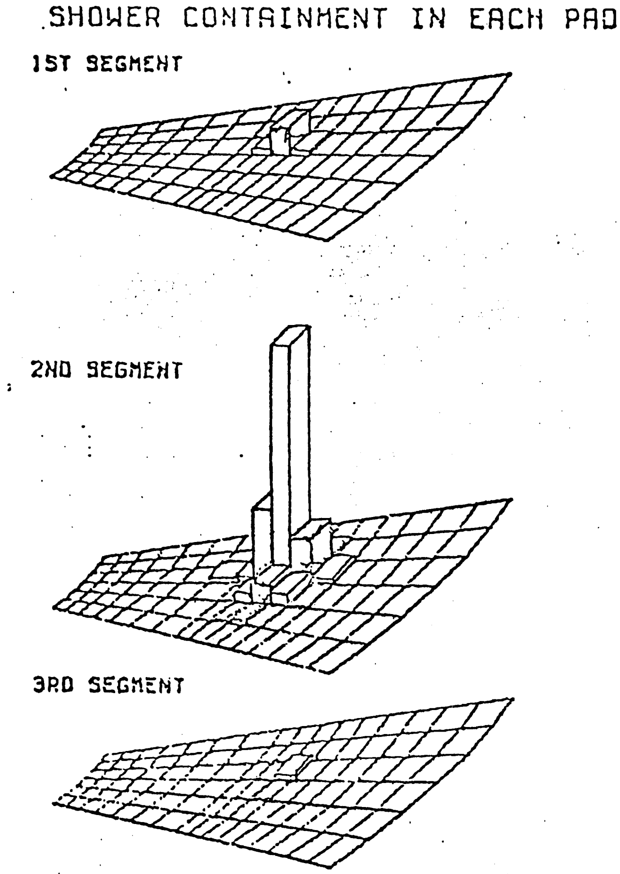

100 GeV π^-

Fig. 26

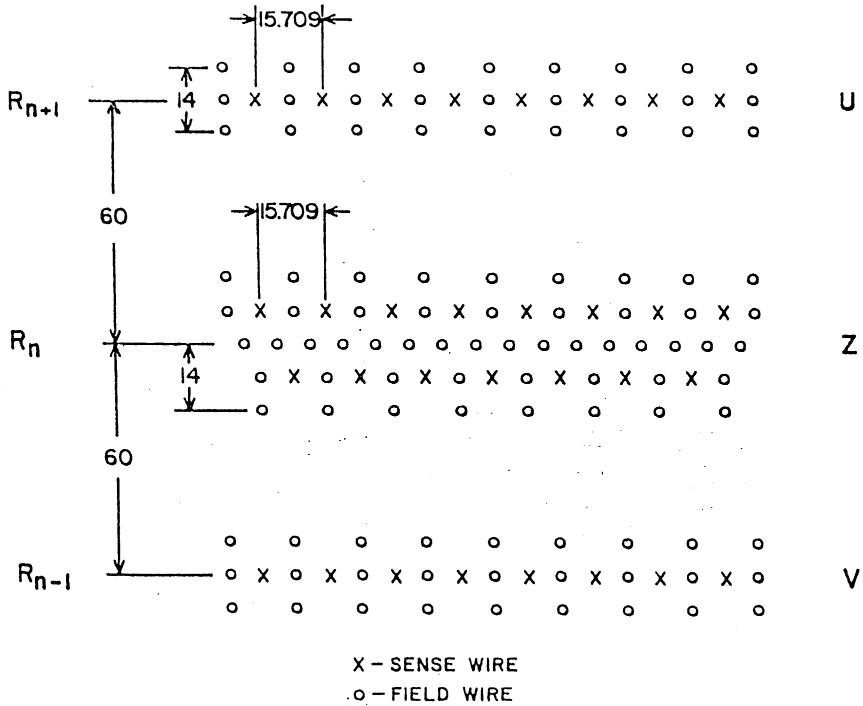

Fig. 27

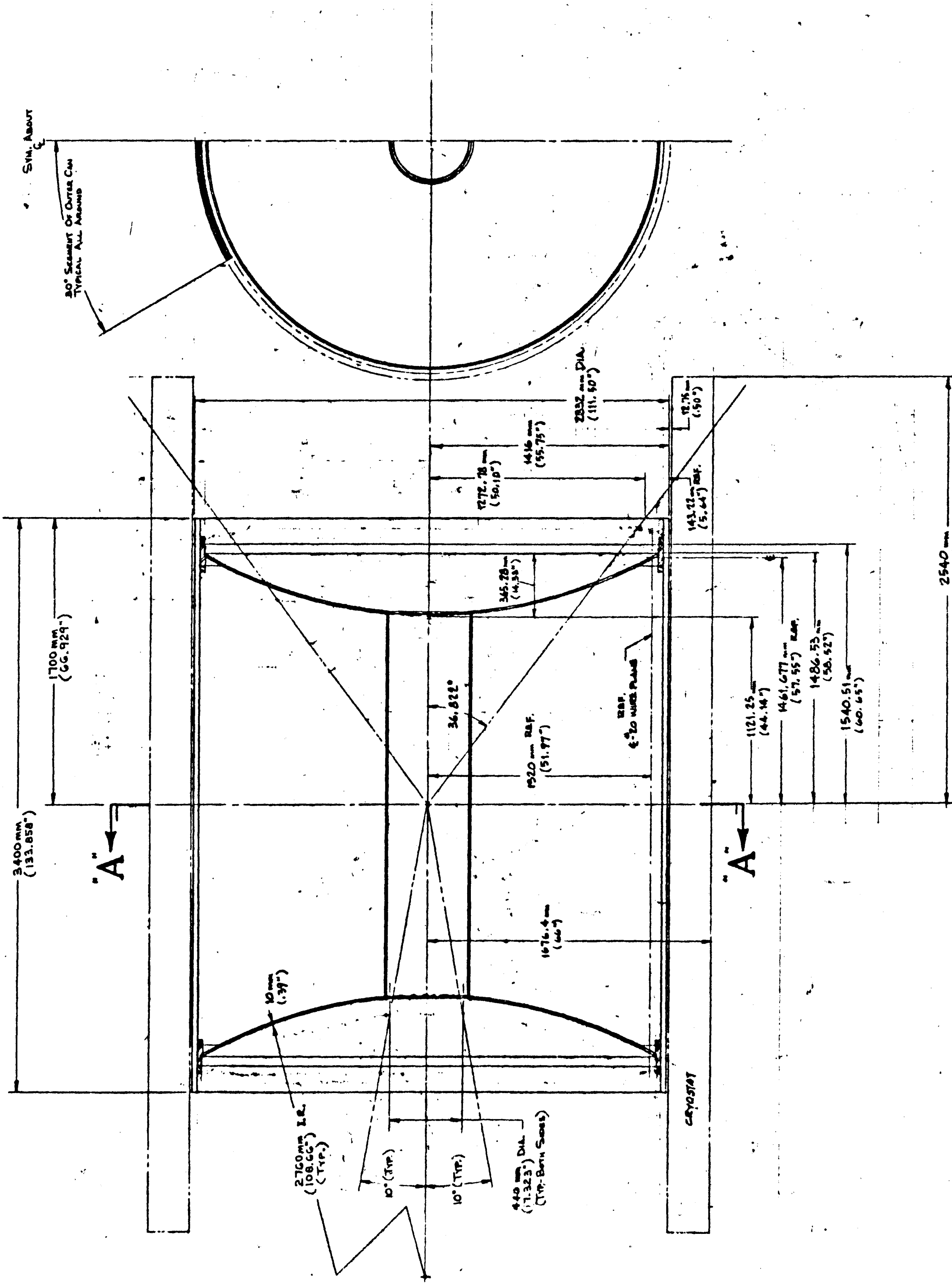
"A"
"A"
3400 mm (133.858")
1700 mm (66.929")
2540 mm (100")
36.822°
CRYOSTAT
10° (TYP.)
10° (TYP.)

Fig. 28

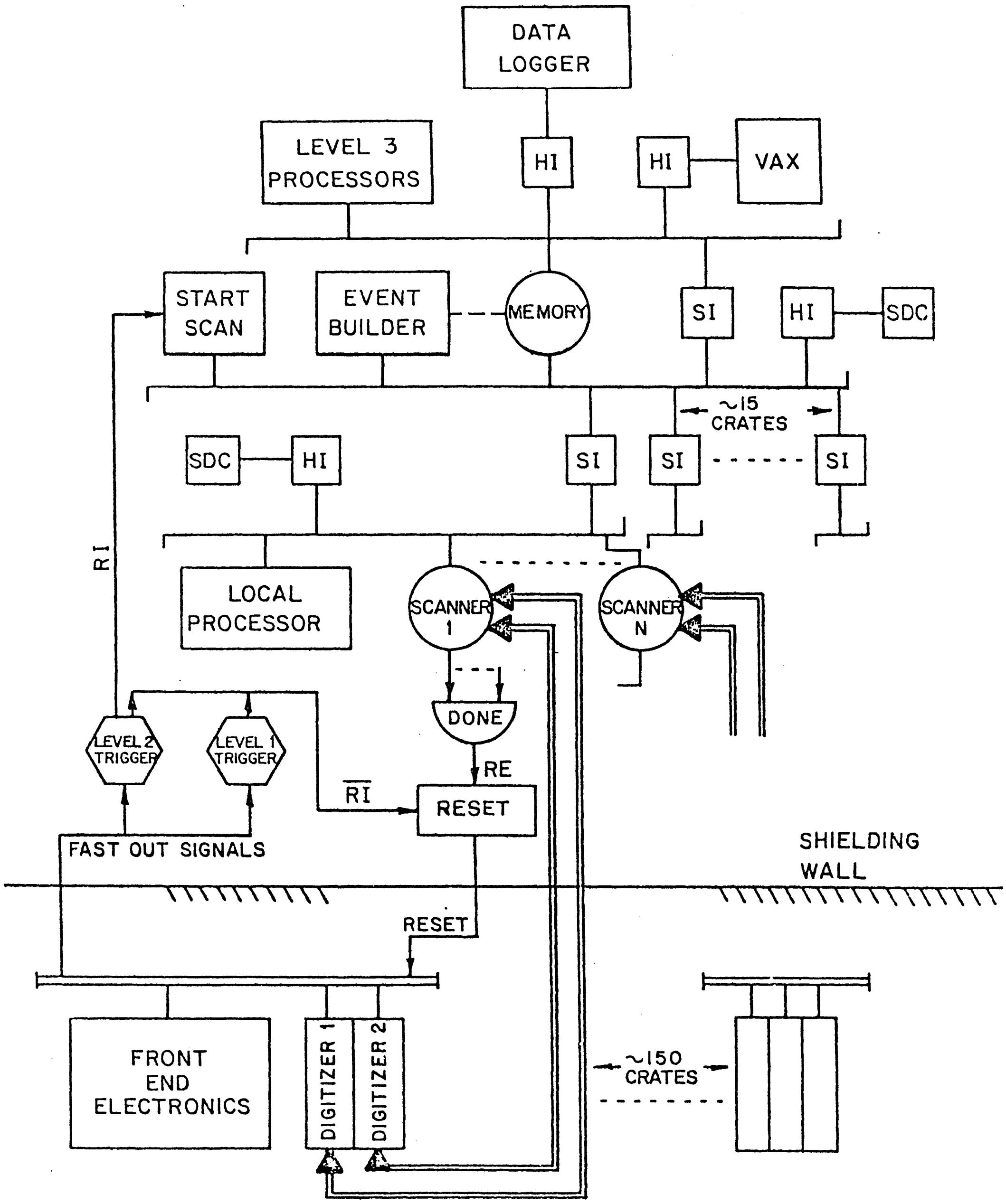

RE RESET ENABLE
RI RESET INHIBIT
HI HOST INTERFACE
SI SEGMENT INTERCONNECT
SDC SERVICE AND DIAGNOSTIC COMPUTER

Fig. 29

Fig. 30

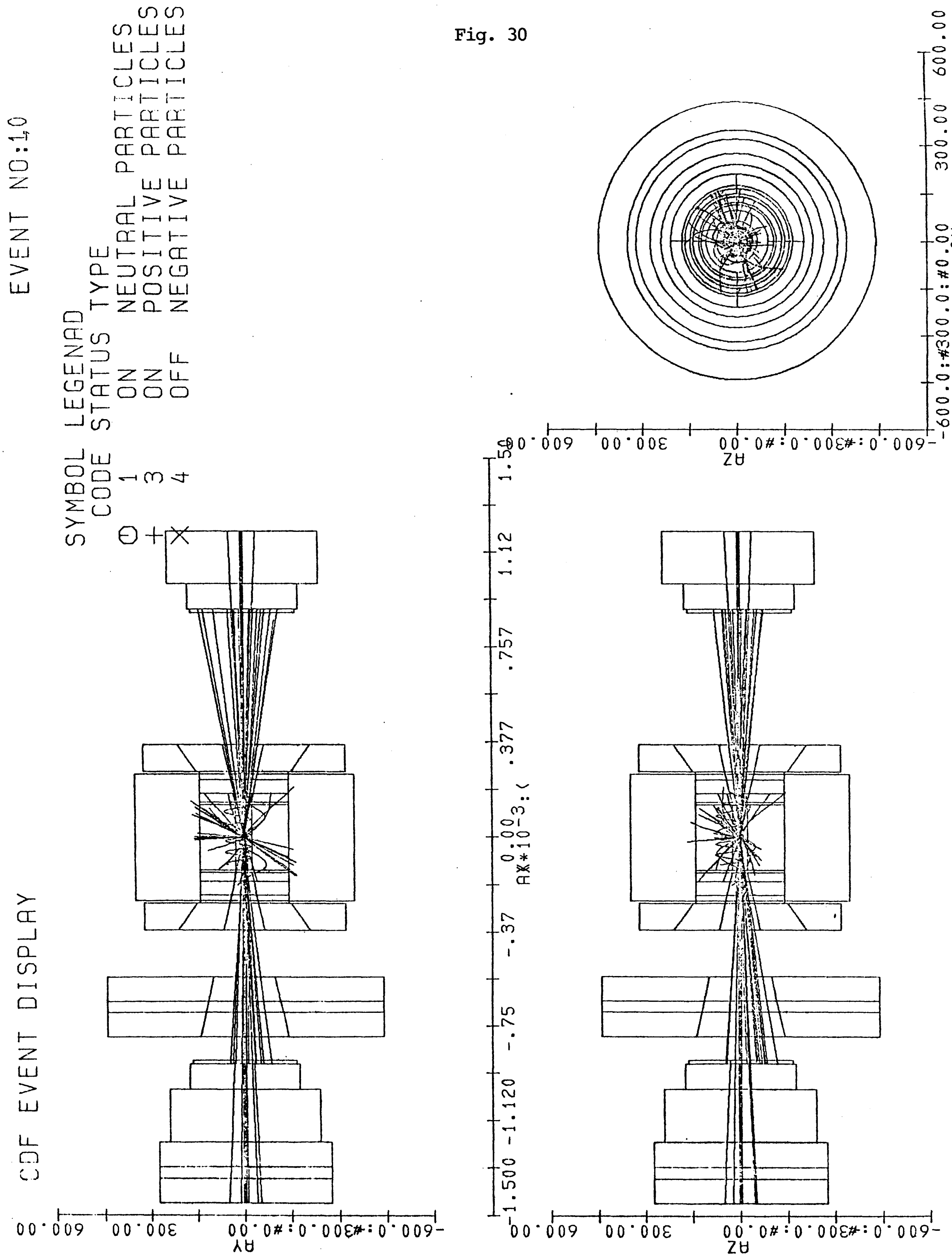
CDF EVENT DISPLAY
EVENT NO:10
SYMBOL LEGENAD
CODE STATUS TYPE
1 ON NEUTRAL PARTICLES
3 ON POSITIVE PARTICLES
4 OFF NEGATIVE PARTICLES
AX*10-3.(
AY
AZ

Fig. 31

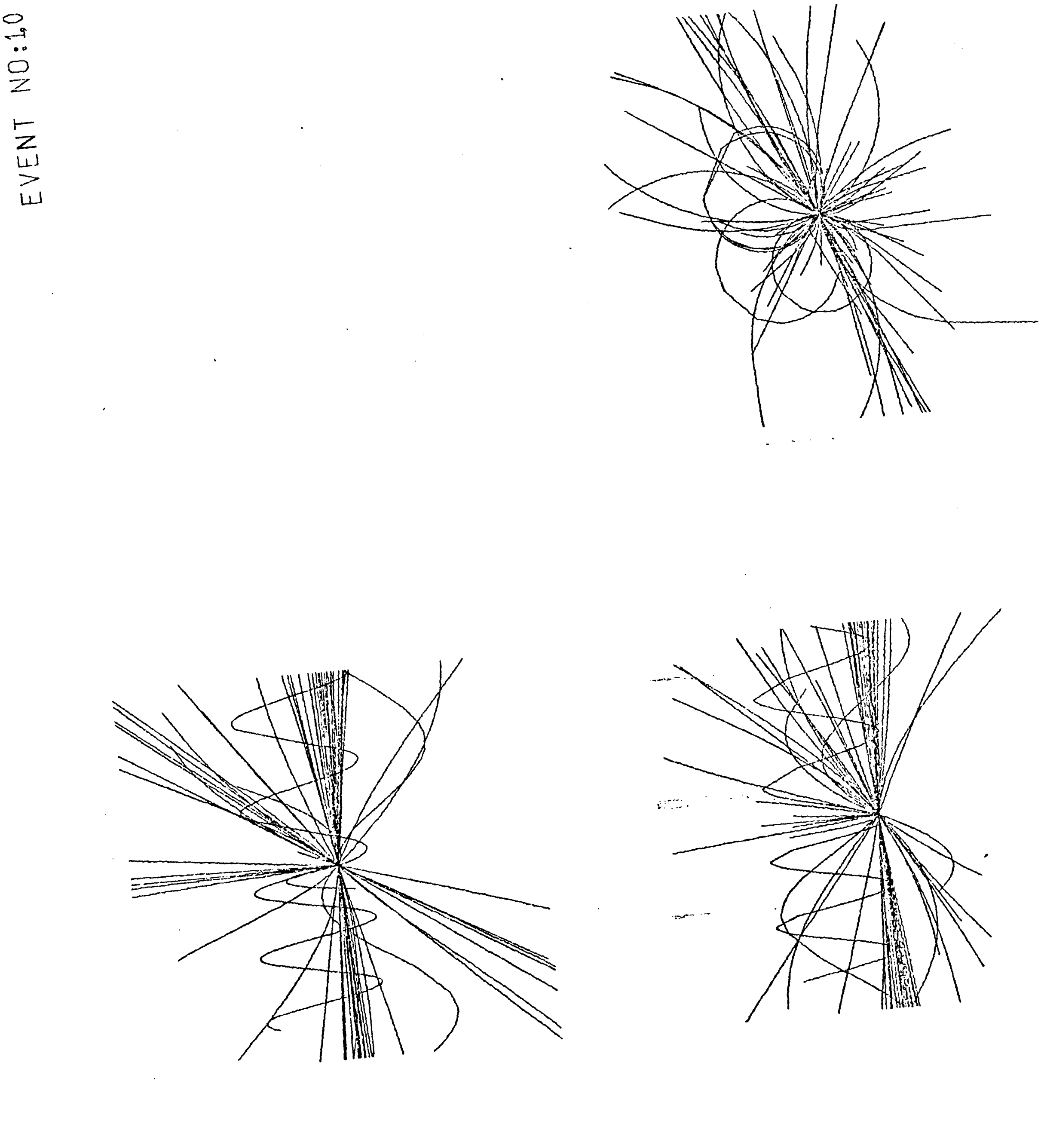

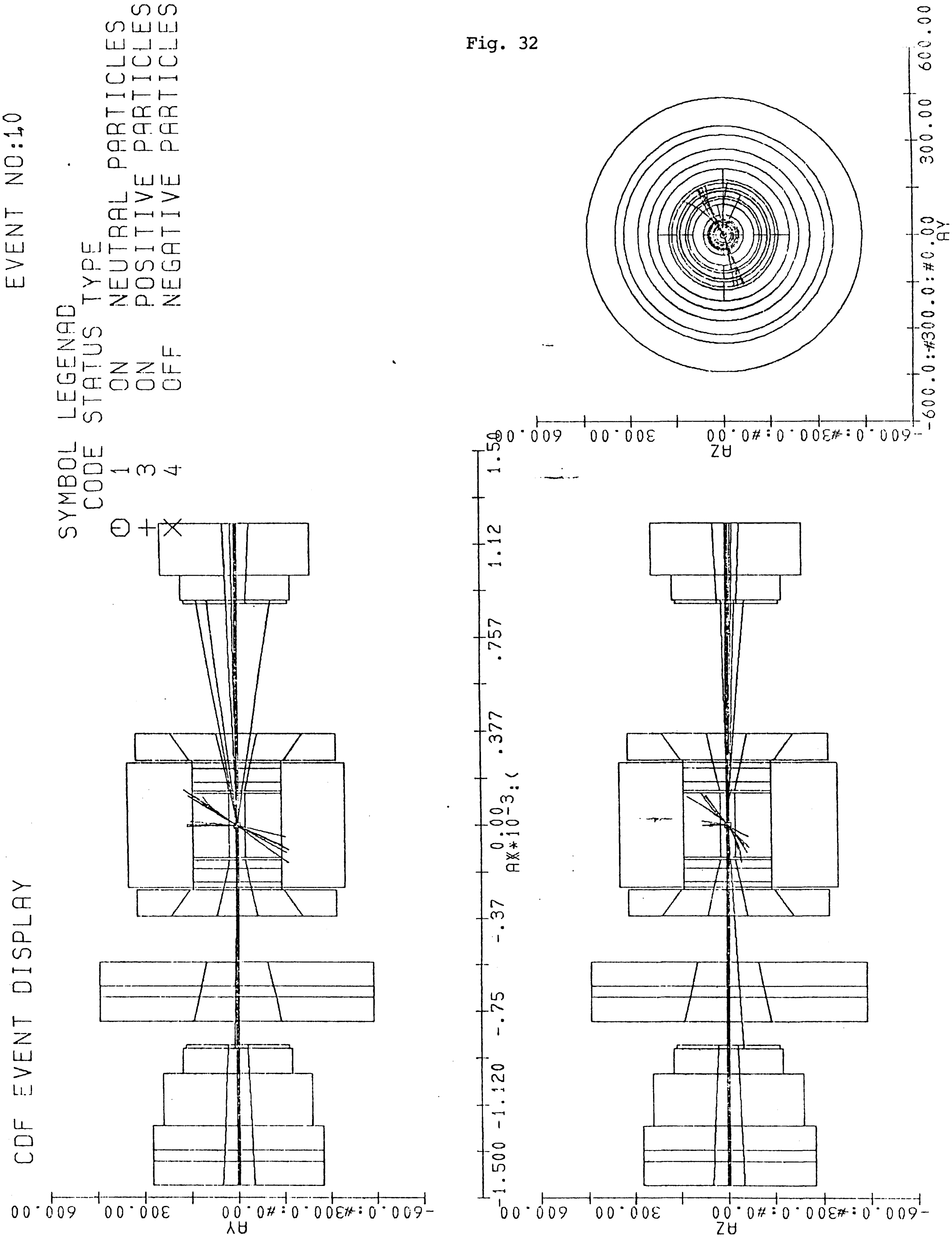
CDF EVENT DISPLAY
EVENT NO:10
SYMBOL LEGENAD
CODE STATUS TYPE
1 ON NEUTRAL PARTICLES
3 ON POSITIVE PARTICLES
4 OFF NEGATIVE PARTICLES
AX*10-3
AY
AZ

Fig. 32

Fig. 33